Covariation of fetal skull and maternal pelvis during the perinatal period in rhesus macaques and evolution of childbirth in primates

Mikaze Kawada[a,1], Masato Nakatsukasa[a], Takeshi Nishimura[b], Akihisa Kaneko[b], and Naoki Morimoto[a,1]

[a]Laboratory of Physical Anthropology, Graduate School of Science, Kyoto University, Kyoto 606-8502, Japan; and [b]Primate Research Institute, Kyoto University, Inuyama, Aichi 484-8506, Japan

Edited by Karen Rosenberg, University of Delaware, Newark, DE, and accepted by Editorial Board Member C. O. Lovejoy July 17, 2020 (received for review February 4, 2020)

A large brain combined with an upright posture in humans has resulted in a high cephalopelvic proportion and frequently obstructed labor. Fischer and Mitteroecker [B. Fischer, P. Mitteroecker, *Proc. Natl. Acad. Sci. U.S.A.* 112, 5655–5660 (2015)] proposed that the morphological covariations between the skull and pelvis could have evolved to ameliorate obstructed labor in humans. The availability of quantitative data of such covariation, especially of the fetal skull and maternal pelvis, however, is still scarce. Here, we present direct evidence of morphological covariations between the skull and pelvis using actual mother–fetus dyads during the perinatal period of *Macaca mulatta*, a species that exhibits cephalopelvic proportions comparable to modern humans. We analyzed the covariation of the three-dimensional morphology of the fetal skull and maternal pelvis using computed tomography-based models. The covariation was mostly observed at the pelvic locations related to the birth canal, and the forms of the birth canal and fetal skull covary in such a way that reduces obstetric difficulties. Therefore, cephalopelvic covariation could have evolved not only in humans, but also in other primate taxa in parallel, or it could have evolved already in the early catarrhines.

skull | pelvis | obstetric dilemma | geometric morphometrics

Encephalization and acquisition of bipedal locomotion are hallmarks of human evolution. In modern humans, adult and neonatal brain volumes reach 1,400 and 400 cc on average, respectively (1–3). Bipedality with upright posture shaped the human pelvis in a specific way compared to other primates. The human pelvis is short and deep along the cephalocaudal and dorsoventral directions, respectively, which is thought to be associated with the stability and efficiency of bipedal locomotion (4–6). The human pelvic morphology results in a narrow birth canal, especially along the anteroposterior direction at the pelvic inlet (7–9). As a result of encephalization and adaptations for bipedalism, neonatal head and maternal pelvic dimensions typically exhibit a tight fit in humans. The large human neonatal head relative to maternal pelvic sizes (a high cephalopelvic proportion) frequently leads to difficulties in childbirth and has prompted a unique delivery process coupled with fetal rotation (refs. 7, 10–13, but see refs. 14, 15).

In principle, the risks of obstructed labor should be reduced by expanding true pelvic dimensions (4, 8, 9, 16, 17). There is a limitation in the capacity of pelvic expansion, however, since increased pelvic width hampers energetic efficiency of bipedal locomotion (refs. 8, 9, 16, 18, but see refs. 19, 20). Such a trade-off that was hypothesized for the human pelvis is known as the "obstetric dilemma" (7, 8, 18, 19, 21–25). This long-standing hypothesis was recently challenged by Warrener et al. (20), who showed that the broader pelves of females compared to males do not result in energetic inefficiency. In either case, the expansion of pelvic dimensions is limited, since a pelvic floor that is too large could increase risk of visceral prolapse (26).

Given the relatively large head of the human neonate and the constrained pelvic width for efficient bipedalism, what could, then, reduce the risk of obstructed labor? Do the morphologies of the skull and pelvis covary and coevolve to reduce difficulty of childbirth? As the delivery process itself is primarily determined by the interaction between the fetal head and maternal pelvis, the morphological covariation between the head and pelvis (cephalopelvic covariation [CPC]) has drawn considerable attention. It has been reported that the sizes of the neonatal and maternal heads show a positive correlation in humans (27, 28). Fischer and Mitteroecker (29) showed that humans with larger heads tend to exhibit a rounder shape of the pelvic inlet with greater projection of the shorter sacrum to the dorsal direction and the larger anteroposterior diameter in the pelvic outlet. They also showed that such covariation between the head size and pelvic shape is stronger in females than in males. Based on these data, they proposed that the morphologies of the skull and pelvis covary to ease childbirth.

Small- to middle-sized primates (e.g., marmosets, squirrel monkeys, macaques, and gibbons) also tend to exhibit high cephalopelvic proportions (7), since maternal body mass and neonatal body and brain masses follow negative allometry (1, 30). In these taxa, the frequency of neonatal death during

Significance

Childbirth is frequently difficult for humans due to a cephalocaudally short and dorsoventrally deep pelvis necessary for upright bipedality and a large neonatal brain. A tight fit between the neonatal head and maternal pelvic dimensions is, however, found not only in humans, but also in some other primate taxa. The rhesus macaques show human-like cephalopelvic proportions. We show that forms of the fetal skull and maternal pelvis during the perinatal period covary in ways to relax the obstructions of childbirth in rhesus macaques. This indicates that morphological covariation of the fetal skull and maternal pelvis could have evolved not only in humans, but also in other primates in parallel, or it could be an example of a catarrhine synapomorphy.

Author contributions: N.M. designed research; M.K., M.N., T.N., A.K., and N.M. performed research; M.K. and N.M. contributed new reagents/analytic tools; M.K. and N.M. analyzed data; M.K., M.N., T.N., and N.M. wrote the paper; and M.K., T.N., A.K., and N.M. acquired data.

The authors declare no competing interest.

This article is a PNAS Direct Submission. K.R. is a guest editor invited by the Editorial Board.

[1]To whom correspondence may be addressed. Email: morimoto@anthro.zool.kyoto-u.ac.jp or kawada@anthro.zool.kyoto-u.ac.jp.

This article contains supporting information online at https://www.pnas.org/lookup/suppl/doi:10.1073/pnas.2002112117/-/DCSupplemental.

First published August 17, 2020.

childbirth is relatively high (4, 10, 25). It is currently unknown whether the CPC evolved only in humans, in parallel in other primate taxa, or is a shared anthropoid synapomorphy. Addressing this question is of special relevance to infer the evolutionary history of the CPC in primates. Here, we assess the CPC in *Macaca*, a genus that exhibits a high cephalopelvic proportion. The macaques exhibit a high cephalopelvic proportion comparable to humans (7, 31, 32), but do not exhibit obligate bipedalism. Investigating the CPC in macaques could thus provide insights into the CPC hypothesis proposed by Fischer and Mitteroecker (29).

While the CPC is the key for understanding the evolution of the delivery processes in primates, our current knowledge is limited in two aspects: First, direct data on the CPC are still scarce (but see ref. 15). Fischer and Mitteroecker (29) proposed the hypothesis based on the within-individual covariation of the skull and pelvis in adults. However, the morphology of the neonatal head is determined not only by the maternal, but also by the paternal genetic factors. Thus, direct phenotypic data of the mother and its fetus are essential. Second, data on the covariation of the three-dimensional neonatal skull and maternal pelvic morphology remain unexplored. In this study, we investigate the CPC using direct data obtained from mother–fetus dyads of rhesus macaques (*Macaca mulatta*) (Fig. 1 and *SI Appendix*, Figs. S1–S3 and Table S1). We obtained detailed skeletal morphological data derived from computed tomography (CT) scans of perinatal rhesus macaques, such that the fetal skull remained physically intact.

We analyzed the CPC using the following framework: First, we identified how the fetal head passes through the birth canal using the in silico simulation. Specifically, we evaluated whether any head rotation is required for the fetuses to pass through the birth canals. In macaques, the diameter of the birth canal is larger dorsoventrally than mediolaterally throughout the birth canal (7, 32–34), while directions of long axes of birth-canal diameters differ at the pelvic inlet and outlet in humans (6, 8, 12, 16). The pattern of fetal rotation in macaques could, thus, differ from that in humans. We virtually moved the three-dimensional surface model of the fetal head relative to that of the maternal pelvis in each of the actual mother–fetus dyads, minimizing contact between the fetal head and maternal pelvis (see also *Materials and Methods*). Second, we asked whether the fetal skull and maternal pelvis show the covariation of three-dimensional morphologies (H0: hypothesis 0). If H0 is supported, we then asked whether the CPC corresponds to childbirth rather than to other functions, such as locomotion (H1: hypothesis 1), and whether the CPC reduces the obstruction of childbirth in rhesus macaques (H2: hypothesis 2). To answer these questions, we assessed the three-dimensional morphologies of the fetal skull and maternal pelvis using geometric morphometrics (*Materials and Methods*).

Results

In all of the mother–fetus dyads examined in this study, the anteroposterior diameter (see *SI Appendix*, Fig. S4 for definition) of the fetal skull was considerably larger than the dorsoventral diameter of the pelvic outlet, and the fetal skull width was considerably larger than the mediolateral diameter of the pelvic outlet (*SI Appendix*, Table S2 and Figs S5 and S6 and Fig. 1). Specifically, the mediolateral diameter of the birth canal was smallest at the ischial spines (*SI Appendix*, Figs. S1, S4, S5, and S6). Thus, the major constraint of childbirth in rhesus macaques is the disproportion of the mediolateral diameters of both the fetal cranium and the pelvic outlet. The in silico simulation showed that the space between the head and birth canal is larger when the fetal face is oriented toward the caudal direction than when it is oriented toward the pubic direction of the mother in all of the dyads (Fig. 1 *B* and *C* and *SI Appendix*, Figs. S5 and S6). When the fetal face was oriented toward the pubic direction of the mother, there were more "crash points" between the fetal skull and maternal pelvis (Fig. 1*B* and *SI Appendix*, Fig. S6). While there were extra spaces ventral and dorsal to the fetal head when the fetal face was oriented toward the caudal direction of the mother (Fig. 1*C* and *SI Appendix*, Fig. S5), further movement and/or rotation of the fetal head was considerably limited (*SI Appendix*, Fig. S5). To minimize the contact of the fetal head and maternal pelvis, the midsagittal planes of the maternal pelvis and fetal skull should, in principle, overlap, and the fetal head should pass through the center of the birth canal (Fig. 1*C*). Thus, it appears that a rotation during childbirth, with

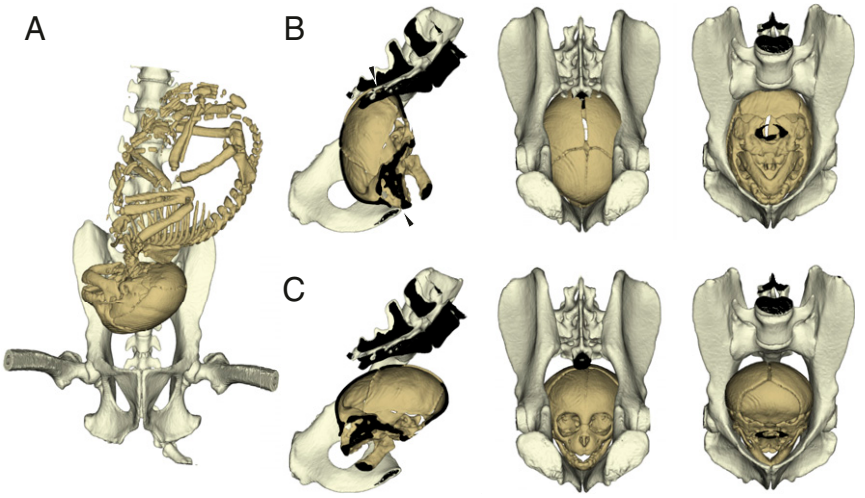

Fig. 1. (*A*) CT-based rendering of the perinatal fetal skeleton and maternal pelvis of rhesus macaques (IDs: PRI-Mm1752 [mother] and PRI-Mm2059 [fetus]). (*B* and *C*) The in silico simulation of the childbirth with the fetal head facing toward the pubic (*B*) and caudal (*C*) directions of the mother (midsagittal section [*Left*], caudal view [*Center*], and superior view [*Right*]). The cephalopelvic proportion is higher at the pelvic outlet than at the pelvic inlet. (*B*) Black arrowheads indicate "crash points," where the fetal head exceeds the dimensions of the maternal birth canal. (*C*) Fetuses that face the caudal direction of the mother result in a lessened risk of obstruction, since the anteroposterior diameter of the head is larger than that of the pelvic inlet. Note that the mediolateral diameter of the fetal head is considerably larger than that of the pelvic outlet of the maternal birth canal. See *SI Appendix*, Figs. S1, S5, and S6 for the simulation of other dyads.

which the fetal head is in oblique or transverse positions relative to the maternal pelvis, is not likely in most of the dyads (11 out of 12; *SI Appendix*, Fig. S5).

To test these hypotheses, we quantified the three-dimensional morphologies of the fetal skull and maternal pelvis by anatomical points of reference (so-called landmarks) (*SI Appendix*, Fig. S7). According to H0, actual mother–fetus dyads should show a higher level of morphological covariation than random combinations of mothers and fetuses. This can be tested by using two-block partial least-squares (PLS; *Materials and Methods*) (35). According to H1, the magnitude of the covariation should be greater at locations within the birth canal (*Materials and Methods*) than other locations of the pelvis. The birth canal of rhesus macaques consists of the *linea terminalis* (the ilium, upper part of the sacrum, and upper part of the pubis; inlet); ischium, sacrum, and pubis (midplane); and the lower part of the ischium and the lower part of the sacrum (outlet). In contrast to humans, the pelvic outlet in nonhuman primates is located dorsal to the ischial tuberosities (10, 36). Thus, the location of the ischial tuberosities, as well as the ischial spines, should be closely associated with difficulty of childbirth in rhesus macaques. Finally, if the CPC reduces the obstruction during childbirth (H2), then locations of the fetal skull and maternal pelvis, especially the birth canal, that contribute to CPC should correspond to each other. For example, it is expected that the covariation will be observed between the overall morphologies of the fetal skull and maternal pelvis; i.e., mothers with birth canals of circular vs. elliptic cross-sectional shape should have fetuses with globular vs. ellipsoidal skulls, respectively.

Test of H0. In this study, we focused on the variation in form (size and shape) (37). The results of two-block PLS showed that the fetal skull and maternal pelvis exhibit a relatively high level of covariation ($RV = 0.60$; $P = 0.02$, level of significance was tested by 10,000 permutations; see Fig. 2 for PLS1 scores) (*Materials and Methods*).

Test of H1. We then evaluated the contribution ratio of each landmark coordinate to PLS1 in the maternal pelvis, which was calculated as the proportion of PLS1-related variance to the entire variance of the coordinate for each landmark (henceforth PLSC [PLS-contribution] score; see *Materials and Methods* for formula). The PLSC score was statistically higher at birth-canal-related landmarks than at other landmarks ($P = 0.01$, Wilcoxon rank sum test). The visualization of the landmark-specific PLSC score (Fig. 3) showed that the contribution ratio was relatively high, especially at the pelvic inlet (e.g., on the pelvic brim, pubic region, and sacral promontory) and at the outlet (e.g., on the medial parts of the pelvic tuberosities and ischial spines). In contrast, the PLSC was relatively low on the lateral parts of the ilium and ischium, which are not directly related to the morphology of the birth canal.

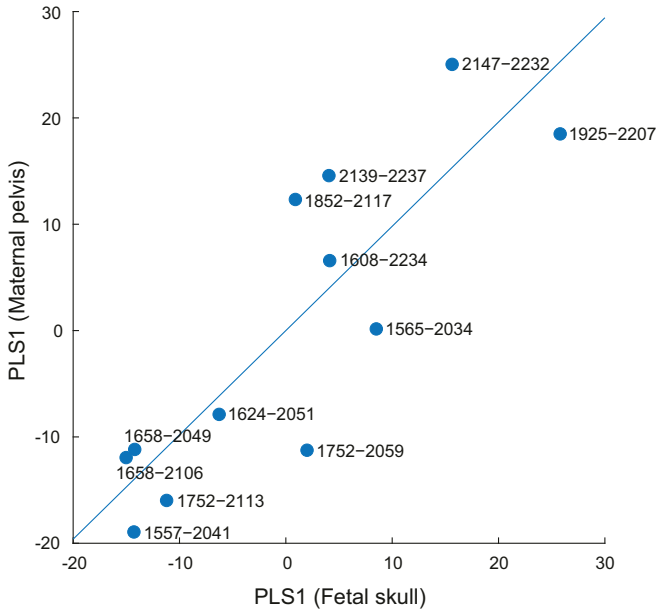

Fig. 2. Plot graph of the PLS1 scores of the fetal skull and maternal pelvis. Numbers indicate IDs of mothers and fetuses (PRI-Mm-numbers).

Test of H2. The morphologies corresponding to highest and lowest PLS1 scores (PLSmax and PLSmin, respectively) were visualized by using thin-plate spline-based morphing of the three-dimensional surface models for the fetal skull and maternal pelvis (Fig. 4). PLSmax and PLSmin correspond to the small and large sizes of the fetal skull and maternal pelvis, respectively. The visualization of PLS1-related morphological variations is summarized as follows.

Skull. The width of the fetal skull is fairly constant for the PLSmax and PLSmin fetal skulls, despite the difference in their overall sizes (Fig. 4*A*). Thus, the overall shape of the PLSmax (small) skull is rounded due to relatively large mediolateral diameter, while that of the PLSmin (large) is anteroposteriorly and superoinferiorly elongated (Fig. 4*A*; see *SI Appendix*, Fig. S8 for measurements of the skull width relative to the overall skull size). Thus, the size variation of the fetal skull is largely due to variation of the length and height, while the skull width remains fairly constant.

Pelvis. The dorsoventral and mediolateral diameters of the pelvic inlet are fairly constant for the PLSmax and PLSmin pelves (Fig. 4*B*). In the PLSmax (small) pelvis, the inferior pubic ramus is more anteriorly positioned relative to the superior pubic ramus, such that the birth canal is relatively wide in the PLSmax (small) pelvis. The ischium spreads laterally, such that the bi-ischial distance is greater relative to the overall size at the outlet in the PLSmax (small) pelvis. Furthermore, the sacrum projects more posteriorly in the PLSmax (small) pelvis. Collectively, the birth canal is large relative to the overall size of the pelvis at both the pelvic inlet and outlet in the PLSmax (small) pelvis (Fig. 4*B*; see *SI Appendix*, Fig. S8 for measurements of diameters of the pelvic inlet and outlet relative to overall pelvic size).

Discussion

Results of the in silico simulation show that the fetal head should change its orientation, such that the face of the fetus is oriented toward the caudal direction rather than to the pubic direction of the mother to ease childbirth (Fig. 1 and *SI Appendix*, Figs. S5 and S6). Thus, head rotation is required for the fetus to pass through the birth canal with less obstruction in rhesus macaques. This is consistent with a field observation of childbirth in black macaques (*Macaca nigra*) (38). Our results are also consistent with findings of Stoller's pioneering study (15) in two respects: The first is the fetal rotation observed in Stoller's study, with dorsal flexion of the fetal head during childbirth in *Papio* that have longer snouts (15). Our data add further evidence to the notion that fetal rotation during childbirth is required not only in primates with long snouts, but also in those with relatively short snouts (rhesus macaques). The second is fetal neck extension. Orienting the face toward the caudal direction of the mother should require neck extension of the fetus. This is consistent with Stoller's finding that neck extension is a way to alleviate obstructed labor in nonhuman primates with high cephalopelvic proportions (15). While these inferences could be drawn from our data, there are two factors that remain to be elucidated, one each on the fetal and maternal side. The first is the temporary deformation of the fetal head. In our sample, 10 out of 12 fetuses

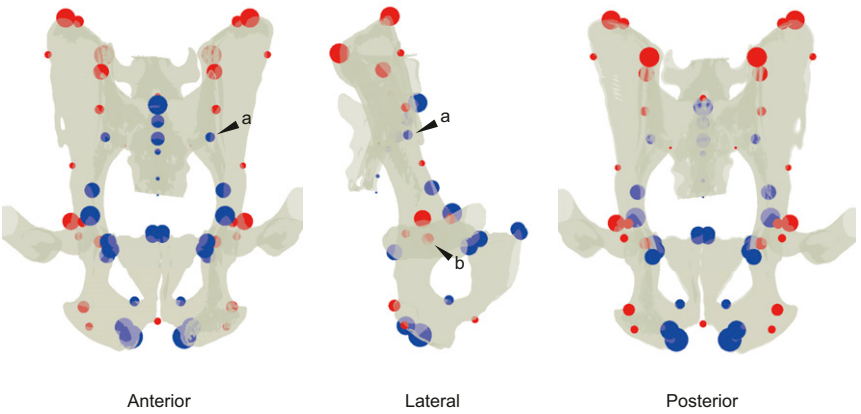

Fig. 3. Visualization of the PLSC scores. The proportion of the PLS1-related variation to total variation is visualized as different-sized spheres (blue, birth canal-related landmarks [see *Materials and Methods* and *SI Appendix*, Table S4 for definition]; red, other locations). The PLSC score is generally high at birth-canal-related locations (with exceptions such as the location indicated by the arrowhead "a"). Conversely, the PLSC score is generally low at locomotion-related locations (e.g., at the acetabulum [indicated by the arrowhead "b"]).

exhibited unfused metopic sutures (with varying degree of fusion; *SI Appendix*, Fig. S2). The unfused metopic suture permits the temporary deformation of the fetal skull (39). Given the narrow width of the pelvic outlet relative to the fetal-skull width (*SI Appendix*, Fig. S5 and Table S2), it is likely that some degree of deformation occurs when the fetus passes through the pelvic outlet. The second is the ligamentary relaxation of the maternal pelvis. The varying degree of the fusion/closure of the metopic suture suggests varying degrees of skull deformation. In cases when the degree of skull deformation during delivery is low, it is the pelvis that should remodel to widen the birth canal (40). Stoller (15) also reported the effect of ligamentary relaxation. With the CT-based data for static condition obtained in this study, direct evaluation of these factors is difficult. Further evaluation by means of real-time tracking of the delivery processes (41) is needed to reveal the actual processes of childbirth in rhesus macaques.

The analyses of the three-dimensional morphologies show that the forms of the fetal skull and maternal pelvis exhibit a relatively high level of covariation (supporting H0) and that the CPC along the PLS1 axes is largely explained by the covariation of the fetal skull and birth canal (Figs. 3 and 4; supporting H1). Furthermore, the direction of the morphological variation was consistent (i.e., along the mediolateral direction) in the fetal skull and maternal pelvis (Fig. 4). The morphological features found in the small-sized (PLSmax) pelvis were consistent with female-specific features of the pelvis that was previously reported in macaques, such as the large dorsoventral diameter of the pelvic inlet and width of the pelvic inlet and outlet (42). This indicates that female-specific features are expressed in the small-sized pelvis to a greater extent. Thus, our data show that the pattern of CPC reduces the risk of obstructed labor, which supports H2.

Collectively, our data provide strong support for the hypothesis that the fetal skull and maternal pelvis exhibit the morphological covariation in order to reduce the risk of obstructed labor in rhesus macaques. The fetal skull and maternal pelvis, however, show some features that do not follow expectations under H1 (CPC to ease childbirth). First, not all of the birth-canal-related locations contribute to CPC. Specifically, the PLSC scores were relatively low at the acetabulum and sacroiliac joints (Fig. 3), even though they are relevant components of the birth canal. Furthermore, the morphological variance was relatively low at these locations (*SI Appendix*, Fig. S9). We hypothesize that CPC-related plasticity is constrained in these locations, since they are also relevant for locomotor function. Increasing biacetabular distance and width of the sacrum would cause an increased width of the trunk, owing to its morphological covariation with the pelvis (43), which could result in increased body weight and reduced locomotor efficiency. Furthermore, an increased biacetabular distance could hamper arboreal locomotor behaviors (44). These inferences are in accordance with the framework of "obstetric dilemma" for pelvic morphology and bipedal locomotion in humans (refs. 8, 9, 16, 18, but see refs. 19, 20). Second, the mediolateral diameter of the fetal skull is constant for small and large skulls (Fig. 4), even though the constant diameter of the fetal skull can contribute to obstructed labor. We hypothesize that the maintenance of a certain diameter of the cranium is relevant for keeping a certain size and shape of the brain during early ontogeny. It has been suggested that the spatial relationship of the craniofacial complex—i.e., basic craniofacial shape— is already established by the fetal period [macaques (45, 46); humans (47–50)]. It is, thus, likely that the large mediolateral diameter of the skull during the fetal period is a developmental requisite. These hypotheses on functional and developmental constraints on the maternal pelvis and the fetal skull should be further tested.

Our data show that the CPC is present in a primate taxon that does not exhibit a specialized locomotor behavior, such as obligate bipedality or extreme encephalization, as modern humans. It appears that the pattern of covariation observed in rhesus macaques is at least partly similar to that in humans. For example, the sacrum is more posteriorly projected in the small-sized pelvis in rhesus macaques (Fig. 4*B*), as observed in human females with short stature (29). On the other hand, the shape of the pelvic inlet is fairly similar in small- and large-sized pelves in rhesus macaques (Fig. 4*B*), while it differs between human females with short and tall stature (29). It is likely that different patterns of the CPC in humans and rhesus macaques reflect different patterns of obstetric constraint. Our data indicate that the CPC could evolve in different ways in each primate taxa, reflecting taxon-specific patterns of obstetric difficulty and locomotor constraint.

The mechanisms behind the observed CPC remain to be elucidated. Fischer and Mitteroecker (29) proposed a correlational selection on the morphologies of the skull and pelvis via genetic linkage due to their proximity in chromosomes and pleiotropic effects of one locus or multiple loci that are unlinked with each other. Our data suggest that such mechanisms at the genetic level could be shared in humans and rhesus macaques. Further studies on genotype–phenotype correlations, from the perspective that the mechanisms of CPC could be shared in humans and macaques, are required to answer these questions.

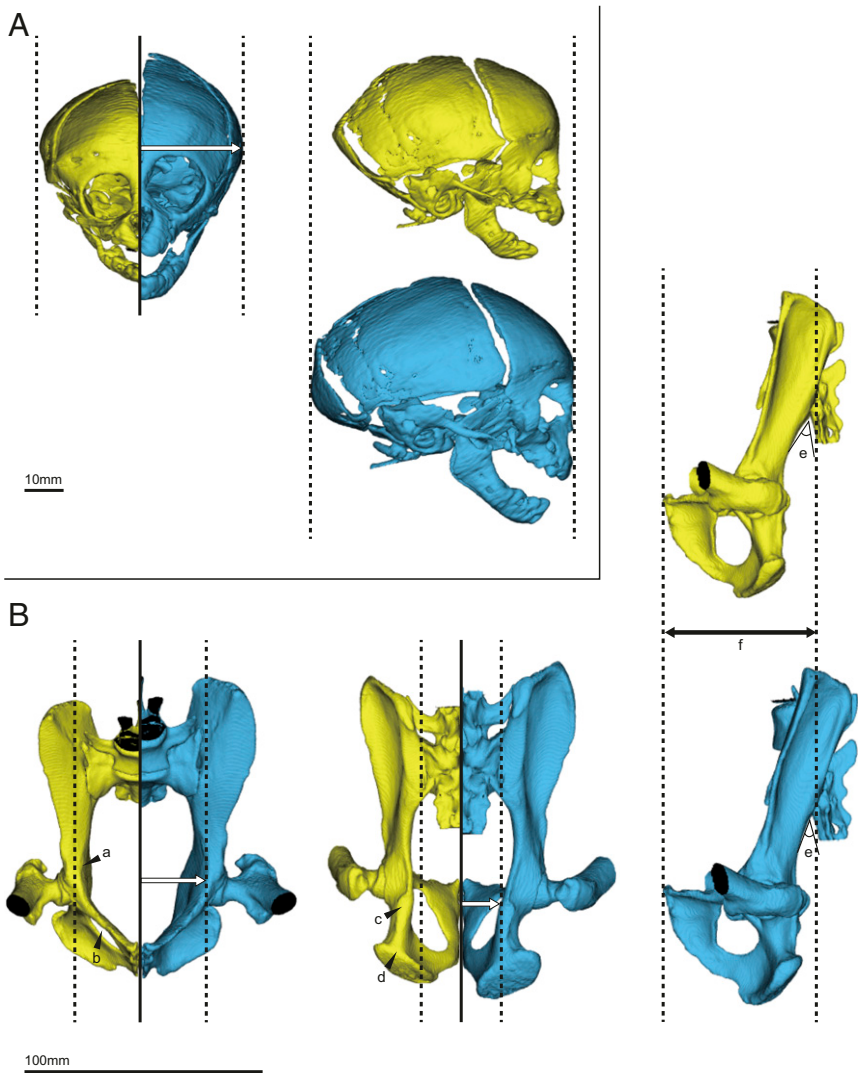

Fig. 4. Morphological variations of the fetal skull (*A*) and maternal pelvis (*B*) along PLS1 axes. The yellow and blue models correspond to PLSmax (small) and PLSmin (large), respectively. The width of the fetal skull and the pelvic inlet remain fairly constant, despite the differences of the overall sizes (*A*, *Left* [fetal skull] and *B*, *Left* [maternal pelvis]; dotted lines and arrows show the width defined in the blue model). (*B*) The small-sized pelvis (yellow) has larger birth-canal dimensions relative to the whole pelvic size than the large-sized pelvis (blue). The markers a–f indicate features of the small-sized pelvis (yellow) compared to the large-sized pelvis (blue). The arrowhead "a" indicates the relative expansion of the width of the pelvic inlet. The arrowhead "b" indicates that the inferior pubic ramus is more anteriorly positioned relative to the superior pubic ramus, such that the pelvic outlet is relatively large (expressed also as visibility of the *foramen obturatum* in this view). The arrowheads "c" and "d" indicate the relative expansion of the pelvic outlet at the ischial spines (c) and ischial tuberosities (d). The angle between the *os coxa* and sacrum is greater (e), which results in the relative expansion of the dorsoventral dimeter of the birth canal (f).

The limited sample size of the present study must be considered in the interpretation of the results, and a detailed evaluation of the questions raised here must await further studies. However, our data showing that the CPC is not unique to humans have broad implications for the study of evolution of childbirth in primates. We have shown that rhesus macaques, which have neither obligate bipedal locomotion nor extreme encephalization as modern humans, exhibit the CPC. This indicates that specialized pelvic morphology and a high degree of encephalization are not necessarily required for the acquisition of the CPC and that the CPC can be more generalized than previously thought. There could be two scenarios for evolution of the CPC that remain to be tested. The first scenario is that the CPC evolved independently in humans and macaques, and possibly in other primates, such as New World monkeys (NWMs) with high cephalopelvic proportions. The alternative scenario is that the CPC evolved in the early catarrhines before the split of the Hominoidea and Cercopithecoidea, or even prior to the divergence of stem catarrhines, given a high degree of cephalopelvic proportions in some NWMs. The latter scenario indicates that the CPC evolved prior to the acquisition of bipedal locomotion and encephalization in the human lineage and may in fact be an anthropoid synapomorphy. These scenarios remain to be tested with a larger sample of primates, especially including taxa with low cephalopelvic proportions, such as great apes. The evaluation of a wider range of primate taxa in future studies is of special relevance to clarify the CPC perspective in the morphological evolution of the skull and pelvis.

Materials and Methods

CT Scanning. Using a medical CT scanner (Asteion, Cannon Medical Systems), we scanned 12 *Macaca mulatta* (rhesus macaques) mother–fetus dyads, of which two mothers were scanned twice with different fetuses in different years (*SI Appendix*, Table S1). Due to the difficulty in obtaining data of mother–fetus dyads, we counted the data from these two mothers as independent

datasets. The rhesus macaques used in this study were all raised at the Primate Research Institute of Kyoto University (KUPRI). All CT scans were performed at KUPRI. The CT scans used here were registered and are available via the website of the Digital Morphology Museum of KUPRI (http://dmm.pri.kyoto-u.ac.jp/dmm/WebGallery/index.html).

Mothers were anesthetized by A.K. before CT scans using one of the following protocols: intramuscularly with 10 mg of ketamine hydrochloride (Ketalar; Daiichi Sankyo Propharma), 0.01 mg of atropine sulfate hydrate (Atropine Injection 0.05%, Terumo, Tokyo, Japan) per kilogram of body weight; or intramuscularly with 8 mg of ketamine hydrochloride or 0.0125 mg of medetomidine hydrochloride (Domitor; Nippon Zenyaku Kogyo). Note that method of anesthetization did not affect quality of resulting images of CT scans. While the subjects were under anesthesia, the pulse rate and SpO_2 (an estimate of arterial oxygen saturation) were monitored by using a medical monitor (BP-608EV, Fukuda Colin Co. Ltd.). Respiration was checked visually. After all of the scanning procedures were completed, subjects that were anesthetized with medetomidine hydrochloride were awakened by an intramuscular injection of 0.03125 mg of atipamezole (Mepatia; Meiji) per kilogram of body weight.

The CT scanning and image-reconstruction parameters were as follows: beam collimation 1.0 mm, pitch: 0.75, reconstruction interval: 0.3–0.5 mm, reconstruction kernel: FC30 or FC31. We controlled the timing of the scan during pregnancy as much as possible, but each dataset has different lengths of time lags between the dates of CT scan and birth, which varied from 8 to 37 d (*SI Appendix*, Table S1). In 10 out of 12 cases, the fetal head was oriented toward the caudal direction of the mother (*SI Appendix*, Fig. S1). The CT volumetric data were then converted into surface models by using Amira (Thermo Fisher Scientific, Version 5.50). All experiments were performed in strict accordance with the Guidelines for the Care and Use of Laboratory Primates at KUPRI (51). The protocol was approved by the Animal Welfare and Animal Care Committee at KUPRI (permits 2013-004, 2015-004, 2018-018, and 2020-156).

Morphometric Data Acquisition and Analysis. The three-dimensional surface models of mother–fetus dyads derived from CT data were imported to an in-house program, ForMATit, developed by N.M. (MATLAB-based [MathWorks, Version R2019b]). The surface models were separated into mothers and fetuses to perform the in silico simulation of childbirth. Various positions and orientations of the fetal head relative to the maternal pelvis were simulated for all of the dyads (Fig. 1 and *SI Appendix*, Figs. S5 and S6).

The three-dimensional morphology was quantified by using landmarks (*SI Appendix*, Fig. S7; a total of 74 and 59 landmarks for the skull and pelvis, respectively) using ForMATit. The landmark locations were determined following ref. 52 for the fetal skull and refs. 42, 53 for the maternal pelvis. See *SI Appendix*, Tables S3 and S4 for landmark definitions (landmark data are compiled in Dataset S1). The overall sizes of the fetal skull and maternal pelvis were evaluated by the centroid size calculated from landmark coordinate data (37). In this study, we focus on the form (size and shape) of the fetal skull and maternal pelvis. Thus, the following analyses of the morphological covariation were performed without size standardization.

The morphological covariation was evaluated by two-block PLS (35), following the protocols in refs. 54, 55. The differences in position and orientation of landmark configuration were corrected by using Generalized Procrustes fitting for each skull and pelvis. The level of covariation between two sets (blocks) of data (here, landmark configurations of the skull and pelvis) was evaluated by *RV* coefficient (56) calculated using the variance–covariance matrix within each block and covariance matrix between the two blocks. Note that *RV* is an extension of the expression for the squared correlation coefficient (54). The level of significance of *RV* was evaluated by using the permutation test (10,000 permutations); that is, a comparison of the *RV* coefficient for actual mother–fetus dyads and that of randomly generated dyads, testing whether the observed covariation is obtained by chance. The *P* value was calculated as the number of RV_{random} that is larger than RV_{real}, divided by the total number of permutations (54).

The contribution ratio of PLS1-related variation to the total variation, which we call PLSC score, was calculated for each landmark as

$$PLSC_i = \frac{\sum_{x,y,z} var(coord_{i,\ PLS1})}{\sum_{x,y,z} var(coord_{i,Proc})},$$

where i denotes the landmark number on the maternal pelvis (i = 1, 2, . . ., 59), *var* denotes the function to calculate the variance, and $coord_{Proc}$ and $coord_{PLS1}$ denote Cartesian coordinates that were processed by Generalized Procrustes fitting and were reconstructed from the PLS1 score for each individual, respectively (thus, the PLSC score at each landmark was calculated from 12 [i.e., sample size of mothers] data points). We then tested whether the PLSC score differed between the birth canal and other locations using the Wilcoxon rank sum test (see *SI Appendix*, Fig. S7 for definition of birth-canal-related landmarks). The PLSC score and variation of landmark coordinates were also visualized as spheres of different sizes plotted on the surface model (Fig. 3).

The morphological variation along the PLS1 axis was visualized for the fetal skull and maternal pelvis as deformations of the surface models at maximum and minimum values of the PLS1 score. The surface models of the skull and pelvis were used as templates for deformation, according to the different landmark configurations, by using thin-plate spline function (57). A dyad, which was close to the average of all individuals, was selected as the template for deformation (IDs: PRI-Mm1565 [mother] and PRI-Mm2034 [fetus]). All of the calculations were performed by using MATLAB.

Data Availability. All data related to this paper are cited in the main text and *SI Appendix*.The CT images used in this study are available on the website of the Digital Morphology Museum of KUPRI (http://dmm.pri.kyoto-u.ac.jp/dmm/WebGallery/). The specimen IDs are provided in *SI Appendix*, Table S1.

ACKNOWLEDGMENTS. We thank the staffs of the Center for Human Evolution Modeling Research at KUPRI for assistance in this study and daily care of the subjects. We also thank W. Morita and S. Kobayashi for giving comments on statistical analyses; B. Shearer for proofreading the manuscript; and the editor and three anonymous reviewers for constructive comments. This study was supported by Cooperative Research Program at KUPRI Grants 2013-B-1, 2015-A-22, and 2018-C-8; and Japan Society for the Promotion of Science KAKENHI Grant 17K07585.

1. J. M. DeSilva, A shift toward birthing relatively large infants early in human evolution. *Proc. Natl. Acad. Sci. U.S.A.* **108**, 1022–1027 (2011).
2. R. A. Foley, P. C. Lee, Ecology and energetics of encephalization in hominid evolution. *Philos. Trans. R. Soc. Lond. B Biol. Sci.* **334**, 223–231, discussion 232 (1991).
3. K. R. Gibson, Evolution of human intelligence: The roles of brain size and mental construction. *Brain Behav. Evol.* **59**, 10–20 (2002).
4. W. Leutenegger, Functional aspects of pelvic morphology in simian primates. *J. Hum. Evol.* **3**, 207–222 (1974).
5. R. G. Tague, C. O. Lovejoy, The obstetric pelvis of A.L. 288-1 (Lucy). *J. Hum. Evol.* **15**, 237–255 (1986).
6. C. O. Lovejoy, The natural history of human gait and posture. Part 1. Spine and pelvis. *Gait Posture* **21**, 95–112 (2005).
7. A. H. Schultz, Sex differences in the pelves of primates. *Am. J. Phys. Anthropol.* **7**, 401–423 (1949).
8. K. Rosenberg, W. Trevathan, Bipedalism and human birth: The obstetrical dilemma revisited. *Evol. Anthropol.* **4**, 161–168 (1995).
9. A. B. Wittman, L. L. Wall, The evolutionary origins of obstructed labor: Bipedalism, encephalization, and the human obstetric dilemma. *Obstet. Gynecol. Surv.* **62**, 739–748 (2007).
10. W. R. Trevathan, Fetal emergence patterns in evolutionary perspective. *Am. Anthropol.* **90**, 674–681 (1988).
11. W. Trevathan, Primate pelvic anatomy and implications for birth. *Philos. Trans. R. Soc. Lond. B Biol. Sci.* **370**, 20140065 (2015).
12. K. Rosenberg, W. Trevathan, Birth, obstetrics and human evolution. *BJOG* **109**, 1199–1206 (2002).
13. J. C. K. Wells, J. M. DeSilva, J. T. Stock, The obstetric dilemma: An ancient game of Russian roulette, or a variable dilemma sensitive to ecology? *Am. J. Phys. Anthropol.* **149** (suppl. 55), 40–71 (2012).
14. S. Hirata, K. Fuwa, K. Sugama, K. Kusunoki, H. Takeshita, Mechanism of birth in chimpanzees: Humans are not unique among primates. *Biol. Lett.* **7**, 686–688 (2011).
15. M. K. Stoller, "The obstetric pelvis and mechanism of labor in nonhuman primates," PhD Thesis, University of Chicago, Chicago, IL (1995).
16. K. R. Rosenberg, The evolution of modern human childbirth. *Am. J. Phys. Anthropol.* **35**, 89–124 (1992).
17. H. Correia, S. Balseiro, M. De Areia, Sexual dimorphism in the human pelvis: Testing a new hypothesis. *Homo* **56**, 153–160 (2005).
18. C. B. Ruff, Biomechanics of the hip and birth in early *Homo*. *Am. J. Phys. Anthropol.* **98**, 527–574 (1995).
19. H. M. Dunsworth, A. G. Warrener, T. Deacon, P. T. Ellison, H. Pontzer, Metabolic hypothesis for human altriciality. *Proc. Natl. Acad. Sci. U.S.A.* **109**, 15212–15216 (2012).
20. A. G. Warrener, K. L. Lewton, H. Pontzer, D. E. Lieberman, A wider pelvis does not increase locomotor cost in humans, with implications for the evolution of childbirth. *PLoS One* **10**, e0118903 (2015).
21. W. M. Krogman, The problem of timing in facial growth, with special reference to period of the changing dentition. *Am. J. Orthod.* **37**, 253–276 (1951).

22. A. M. Roberts, S. K. S. Thorpe, Challenges to human uniqueness: Bipedalism, birth and brains. *J. Zool.* **292**, 281–289 (2014).
23. S. L. Washburn, Tools and human evolution. *Sci. Am.* **203**, 63–75 (1960).
24. A. Huseynov *et al*., Developmental evidence for obstetric adaptation of the human female pelvis. *Proc. Natl. Acad. Sci. U.S.A.* **113**, 5227–5232 (2016).
25. W. Leutenegger, "Encephalization and obstetrics in primates with particular reference to human evolution" in *Primate Brain Evolution: Methods and Concepts*, E. Armstrong, D. Falk, Eds. (Springer US, Boston, MA, 1982), pp. 85–95.
26. E. H. M. Sze, N. Kohli, J. R. Miklos, T. Roat, M. M. Karram, Computed tomography comparison of bony pelvis dimensions between women with and without genital prolapse. *Obstet. Gynecol.* **93**, 229–232 (1999).
27. J. H. Gilmore *et al*., Genetic and environmental contributions to neonatal brain structure: A twin study. *Hum. Brain Mapp.* **31**, 1174–1182 (2010).
28. D. J. A. Smit *et al*., Heritability of head size in Dutch and Australian twin families at ages 0-50 years. *Twin Res. Hum. Genet.* **13**, 370–380 (2010).
29. B. Fischer, P. Mitteroecker, Covariation between human pelvis shape, stature, and head size alleviates the obstetric dilemma. *Proc. Natl. Acad. Sci. U.S.A.* **112**, 5655–5660 (2015).
30. J. M. DeSilva, J. J. Lesnik, Brain size at birth throughout human evolution: A new method for estimating neonatal brain size in hominins. *J. Hum. Evol.* **55**, 1064–1074 (2008).
31. W. Trevathan, *Human Birth: An Evolution Perspective*, (Aldine De Gruyter, New York, 1987).
32. A. H. Schultz, *The Life of Primates*, (Universe Books, New York, NY, 1969).
33. R. G. Tague, Commonalities in dimorphism and variability in the anthropoid pelvis, with implications for the fossil record. *J. Hum. Evol.* **21**, 153–176 (1991).
34. S. L. Washburn, Skeletal proportions of adult langurs and macaques. *Hum. Biol.* **14**, 444 (1942).
35. F. J. Rohlf, M. Corti, Use of two-block partial least-squares to study covariation in shape. *Syst. Biol.* **49**, 740–753 (2000).
36. C. Berge, R. Orban-Segebarth, P. Schmid, Obstetrical interpretation of the australopithecine pelvic cavity. *J. Hum. Evol.* **13**, 573–587 (1984).
37. F. Bookstein, *Morphometric Tools for Landmark Data: Geometry and Biology*, (Cambridge University Press, Cambridge, UK, 1991).
38. J. Duboscq, C. Neumann, D. Perwitasari-Farajallah, A. Engelhardt, Daytime birth of a baby crested black macaque (*Macaca nigra*) in the wild. *Behav. Processes* **79**, 81–84 (2008).
39. D. Falk, C. P. E. Zollikofer, N. Morimoto, M. S. Ponce de León, Metopic suture of Taung (*Australopithecus africanus*) and its implications for hominin brain evolution. *Proc. Natl. Acad. Sci. U.S.A.* **109**, 8467–8470 (2012).
40. N. M. Laudicina, M. Cartmill, "Obstetric constraints in large-brained cebids and modern humans: A comparison of coping mechanisms" in *The 88th Annual Meeting of the American Association of Physical Anthropologists*, (Wiley, New York, NY, 2019), p. 137.
41. O. Ami *et al*., Three-dimensional magnetic resonance imaging of fetal head molding and brain shape changes during the second stage of labor. *PLoS One* **14**, e0215721 (2019).
42. E. A. Moffett, Dimorphism in the size and shape of the birth canal across anthropoid primates. *Anat. Rec. (Hoboken)* **300**, 870–889 (2017).
43. N. Torres-Tamayo *et al*., The torso integration hypothesis revisited in *Homo sapiens*: Contributions to the understanding of hominin body shape evolution. *Am. J. Phys. Anthropol.* **167**, 777–790 (2018).
44. D. M. Badoux, "An introduction to biomechanical principles in primate locomotion and structure" in *Primate Locomotion*, F. A. Jenkins Jr., Ed. (Elsevier, Amsterdam, Netherlands, 1974), pp. 1–43.
45. J. E. Sirianni, L. Newell-Morris, Craniofacial growth of fetal *Macaca nemestrina*: A cephalometric roentgenographic study. *Am. J. Phys. Anthropol.* **53**, 407–421 (1980).
46. J. E. Sirianni, D. R. Swindler, *Growth and Development of the Pigtailed Macaque*, (CRC Press LLC, Boca Raton, FL, 1985).
47. A. R. Burdi, Cephhalometric growth analyses of the human upper face region during the last two trimesters of gestation. *Am. J. Anat.* **125**, 113–122 (1969).
48. M. I. Houpt, Growth of the craniofacial complex of the human fetus. *Am. J. Orthod.* **58**, 373–383 (1970).
49. C. L. B. Lavelle, An analysis of foetal craniofacial growth. *Ann. Hum. Biol.* **1**, 269–287 (1974).
50. M. J. Trenouth, The relationship between differences in regional growth rates and changes in shape during human fetal craniofacial growth. *Arch. Oral Biol.* **30**, 31–35 (1985).
51. Primate Research Institute, Kyoto University, *Guide for the Care and Use of Laboratory Primates*, (Primate Research Institute, Kyoto Univ., Inuyama, Japan, 3rd Ed., 2010).
52. N. Morimoto, N. Ogihara, K. Katayama, K. Shiota, Three-dimensional ontogenetic shape changes in the human cranium during the fetal period. *J. Anat.* **212**, 627–635 (2008).
53. C. P. E. Zollikofer, M. Scherrer, M. S. Ponce de León, Development of pelvic sexual dimorphism in hylobatids: Testing the obstetric constraints hypothesis. *Anat. Rec. (Hoboken)* **300**, 859–869 (2017).
54. C. P. Klingenberg, Morphometric integration and modularity in configurations of landmarks: Tools for evaluating a priori hypotheses. *Evol. Dev.* **11**, 405–421 (2009).
55. M. L. Zelditch, D. L. Swiderski, H. D. Sheets, "Partial least squares analysis" in *Geometric Morphometrics for Biologists, A Primer* (Academic Press, Amsterdam, Netherlands, ed. 2, 2012), pp. 169–188.
56. Y. Escoufier, Le traitement des variables vectorielles. *Biometrics* **29**, 751–760 (1973).
57. C. P. E. Zollikofer, M. S. Ponce De León, Visualizing patterns of craniofacial shape variation in *Homo sapiens*. *Proc. Biol. Sci.* **269**, 801–807 (2002).